Baku State University: Journal of Physics & Space Sciences, **2025**, v2 (4), pp. 11-22

journal homepage: http://bsuj.bsu.edu.az/en

Comprehensive analysis of asymmetric AgNPs/PVA/Ag_2S nanocomposites: influence of silver nitrate concentration on structural and optical properties via vapor-phase sulfidation

Fatma I. Ismayilova*, Mustafa B. Muradov, Goncha M. Eyvazova

Nano Research Laboratory, Baku State University, Baku, Azerbaijan,
Received 25-Aug-2025; Accepted 15-Oct-2025
DOİ: https://doi.org/10.30546/209501.101.2025.2.04.0104

Abstract

In this study, silver nanoparticles (AgNPs) were synthesized via a chemical reduction method and subsequently mixed with polyvinyl alcohol (PVA) polymer. The resulting mixture was air-dried under ambient conditions. AgNPs/PVA nanocomposites with molar concentrations of 0.33 mmol/g, 0.63 mmol/g, and 0.90 mmol/g were successfully fabricated through a solution casting method. The upper surface of the prepared samples was then exposed to hydrogen sulfide (H_2S) gas, leading to the formation of asymmetric structures. The formation and characteristics of these structures were found to depend on the concentration of AgNPs within the nanocomposite and the depth of H_2S penetration into the layers. The structural and optical properties of the resulting asymmetric structures were thoroughly analyzed. Structural changes were investigated using X-ray diffraction (XRD), while optical properties were characterized using ultraviolet-visible (UV-Vis) spectroscopy. A simple sulfidation process involving H_2S gas was applied for the first time to AgNPs/PVA nanocomposites. The analysis of the surface properties revealed significant changes in physical characteristics after sulfidation. Ultimately, the successful formation of AgNPs/PVA/Ag_2S anisotropic structures was achieved, demonstrating the effectiveness of this method for tuning the structural and optical properties of nanocomposite materials.

Keywords: Nanocomposite, Sulfidation, X-ray Diffraction, Surface Plasmon Resonance.
PACS Numbers: 61.46.+w, 73.63.−b, 78.67.−n, 79.60.Jv

* *Corresponding author* – Tel.: (+994) 50 305 96 02
e-mail: fatmaismayilova655@gmail.com; ORCID ID: 0009-0000-4159-128X

1. Introduction

In recent years, the investigation and application of nanomaterials have attracted significant interest across various scientific and technological fields. Among these materials, silver nanoparticles (AgNPs) hold a prominent position due to their unique optical, electrical, and antibacterial properties [1].

The surface plasmon resonance, high conductivity, and nanoscale dimensions of these particles make them promising components in electronics, photonics, medical applications, and sensor technologies. The synthesis of AgNPs in combination with various carrier polymers—particularly polyvinyl alcohol (PVA)—allows for the formation of more stable and functional nanocomposites. In such nanocomposites, the behavior of silver ions, phase composition, and morphological features are among the key factors determining their application potential [2].

Therefore, the sulfidation of AgNP/PVA-based structures and the investigation of the influence of various parameters—especially the concentration of silver nitrate—on this process is of both scientific and technological relevance. The choice of synthesis method for nanocomposite materials directly affects both their structural characteristics and functional properties [3].

Among these methods, vapor-phase sulfidation is considered an effective approach, offering high homogeneity and controllable structural modification. However, studies in the literature regarding the properties of AgNP/PVA/Ag_2S-based asymmetric nanocomposites synthesized via this method are either incomplete or limited to specific concentration ranges of silver nitrate [4].

This gap highlights the necessity for new and comprehensive research in this area. Furthermore, the interpretation of changes in diffraction patterns and structural evolution of multiphase structures synthesized from AgNPs remains an important issue. The primary objective of this research is to investigate the effect of initial silver nitrate concentration on the crystalline structure of asymmetric AgNP/PVA/Ag_2S nanocomposites synthesized via vapor-phase sulfidation, and to analyze their phase composition through X-ray diffraction (XRD) techniques. For this purpose, nanocomposites were prepared using different molar concentrations of silver nitrate (17.66 mM, 35.32 mM, and 52.98 mM), and their crystalline properties were evaluated using XRD analysis.

The results revealed that the initial concentration of silver ions significantly affects both the crystallinity of the nanocomposites and the quantity of the Ag_2S phase. Moreover, based on the obtained data, optimal conditions have been proposed for tuning the structural changes resulting from variations in silver nitrate concentration.

2. Experimental methodology

2.1 Synthesis of AgNPs

One of the most commonly used methods for the synthesis of silver nanoparticles (AgNPs) is the chemical reduction method [5]. This method is widely applied due to its relatively simple technological requirements and low cost [6]. The reduction process is characterized by the transformation of silver ions (Ag^+) into metallic silver (Ag^0) through electron gain. Silver nanoparticles were synthesized via chemical reduction using sodium borohydride ($NaBH_4$) as the reducing agent and polyvinyl alcohol (PVA) as the stabilizer. For the synthesis, 0.32 g of PVA was dissolved in 10 mL of distilled water by heating in a water bath at 60 °C until fully dissolved. Separately, 0.03 g of $AgNO_3$ and 0.004 g of $NaBH_4$ were each dissolved in 10 mL of distilled water. The $AgNO_3$ and $NaBH_4$ solutions were then simultaneously added dropwise (approximately one drop per second) to the PVA solution under continuous stirring. Upon mixing, Ag^+ ions were reduced by $NaBH_4$, leading to the formation of monodisperse AgNPs in the aqueous medium. The reaction can be represented by the following simplified chemical equation:

$$2AgNO_3 + 2NaBH_4 \rightarrow 2Ag + H_2 + B_2H_6 + 2NaNO_3 \quad (1)$$

In this reaction, $NaBH_4$ decomposes to produce gaseous by-products such as hydrogen (H_2) and diborane (B_2H_6). To prevent nanoparticle aggregation and ensure good dispersion during the reduction process, polyvinyl alcohol (PVA) is used as a stabilizing agent. PVA also forms a protective layer that maintains colloidal stability and inhibits the agglomeration of the particles.

2.2. Preparation and sulfidation process of AgNPs/PVA

AgNPs/PVA nanocomposites were fabricated via a facile solution-based method. Initially, a 5 wt% solution of polyvinyl alcohol (PVA) was prepared by dissolving PVA in deionized water under continuous stirring. Subsequently, silver nanoparticles (AgNPs) with three different molar concentrations (17.66 mM, 35.32 mM, and 52.98 mM) were added to the PVA solution. The resulting mixtures were subjected to sonication for 3 minutes to ensure uniform dispersion of nanoparticles. The homogeneous mixtures were then cast into Petri dishes and allowed to air-dry at room temperature for 7 days. As a result, three AgNPs/PVA thin films were obtained with AgNP concentrations of 0.33 mmol/g, 0.63 mmol/g, and 0.90 mmol/g, respectively. The prepared films were then exposed to hydrogen sulfide (H_2S) gas. For this purpose, 4 g of sodium sulfide (Na_2S) was placed in each of three separate sealed containers. The lids of these containers were covered with the AgNPs/PVA nanocomposite films. Then, 10 mL of hydrochloric acid (HCl) solution was added dropwise to

each container over a period of 30 minutes. The purpose of this process was to obtain asymmetric structures through the formation of Ag_2S layers within the nanocomposite films. H_2S gas was generated based on the following reaction:

$$Na^2S + 2HCl \rightarrow 2NaCl + H^2S \uparrow. \quad (2)$$

The produced H_2S gas diffused into the surface of the nanocomposite and reacted with AgNPs, resulting in the formation of Ag_2S. The thickness of the resulting sulfide layer depended on the exposure time to H_2S gas and its penetration depth. Due to the use of AgNPs with varying concentrations, the formed sulfide layers exhibited non-uniformity, which led to the development of asymmetric structural properties in the nanocomposites.

3. Experimental results and their discussion

The X-ray diffraction (XRD) analysis provides crucial insight into the crystalline structure and phase purity of the silver nanoparticles (AgNPs) synthesized using aqueous $AgNO_3$ solutions of varying molar concentrations. As illustrated in Figure 1, the XRD patterns reveal the presence of well-defined diffraction peaks at approximately $2\theta \approx 38.69°$, 45.01°, 65.02°, and 77.90°, which correspond to the (111), (200), (220), and (311) crystallographic planes of face-centered cubic (FCC) silver, respectively. These peaks are consistent with the standard reference data for metallic silver (JCPDS card No. 04-0783) [7], thereby confirming the successful formation of crystalline AgNPs with high phase purity.

For the sample synthesized with the lowest $AgNO_3$ concentration (17.66 mM), only two distinct diffraction peaks are observed at $2\theta \approx 38.69°$ and 65.02°, corresponding to the (111) and (220) planes. The emergence of these peaks confirms the nucleation and initial crystallization of silver nanoparticles even at a low precursor concentration. As the precursor concentration increases to 35.32 mM, a new diffraction peak appears at $2\theta \approx 45.01°$, attributed to the (200) plane. This observation suggests enhanced crystal growth and improved structural ordering as more Ag^+ ions become available during the reduction process. At the highest concentration (52.98 mM), the XRD pattern exhibits all four characteristic peaks of FCC silver, including a newly emerged peak at $2\theta \approx 77.90°$, corresponding to the (311) plane. The progressive appearance and increasing intensity of these diffraction peaks with higher $AgNO_3$ concentrations clearly indicate a significant improvement in the degree of crystallinity and long-range order of the synthesized nanoparticles.

Additionally, the relative broadening of the (111) peak at intermediate and higher concentrations may suggest an increase in crystallite size, which could be attributed to accelerated nucleation and growth dynamics under higher precursor concentrations. The correlation between increased peak intensity and sharper peak

profiles further supports the notion of enhanced crystallinity and particle growth. In summary, the XRD data confirm that silver nanoparticles with a well-defined FCC crystalline structure have been successfully synthesized. The systematic variation in diffraction peak intensity and width with increasing $AgNO_3$ concentration highlights the critical influence of precursor molarity on nanoparticle crystallinity and size. These findings are consistent with previously reported studies and provide a solid foundation for tuning nanoparticle properties via controlled synthesis parameters.

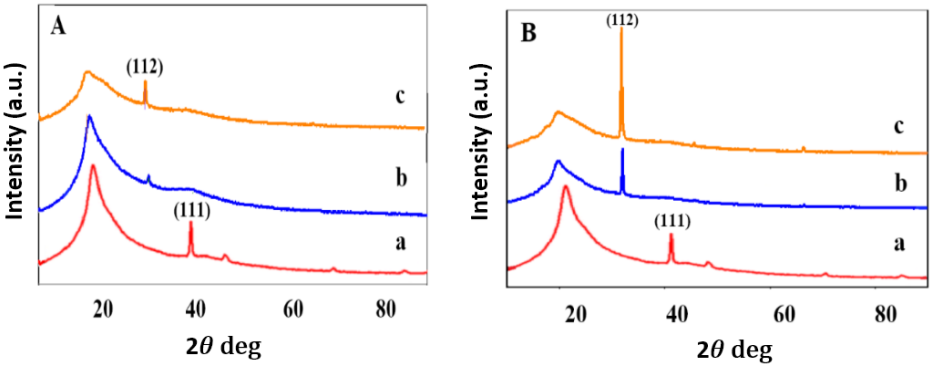

Fig. 1. X-ray diffraction patterns of AgNPs synthesized at molar concentrations of 17.66 mM (a), 35.32 mM (b), and 52.98 mM (c).

Figure 2.A,B(b,c) presents the X-ray diffraction (XRD) patterns of two surfaces of the AgNPs-PVA nanocomposite samples containing AgNPs with concentrations of 0.33 mmol/g and 0.63 mmol/g, respectively. Figure 2.A(a) shows the XRD pattern of the pristine AgNPs-PVA nanocomposite, which was not exposed to H_2S gas (JCPDS No. 04-0783) [7]. As observed, in contrast to the spectrum obtained from the surface directly exposed to H_2S gas, the characteristic peak indexed as (112) for Ag_2S is not present in the spectrum of the surface exposed to air. Notably, a new diffraction peak corresponding to the (112) plane appears at $2\theta = 32.6°$, which is attributed to the formation of Ag_2S on the surface of AgNPs as a result of H_2S gas exposure (JCPDS No. 14-0072) [8].

Furthermore, Figure 2.A,B(c) presents the X-ray diffraction (XRD) patterns of both the top and bottom surfaces of the AgNPs-PVA sample with a silver concentration of 0.63 mmol/g. As clearly observed, the intensity of the (112) diffraction peak—corresponding to the Ag_2S phase formed upon exposure to hydrogen sulfide (H_2S) gas—increases with the rising concentration of silver within the nanocomposite. This enhancement in peak intensity can be attributed to the increased availability of Ag^+ ions, which readily react with H_2S gas according to reaction (2), leading to the formation of a greater quantity of Ag_2S. The formation of the Ag_2S phase

occurs through two distinct diffusion mechanisms: bulk diffusion and surface diffusion. Among these, surface diffusion is typically faster, whereas bulk diffusion proceeds more slowly. Consequently, in the XRD pattern obtained from the top surface of the nanocomposite, the characteristic peaks of Ag_2S are not prominently visible. This absence is due to the relatively limited penetration of H_2S gas into the deeper layers of the material, resulting in a restricted formation of Ag_2S within the bulk.

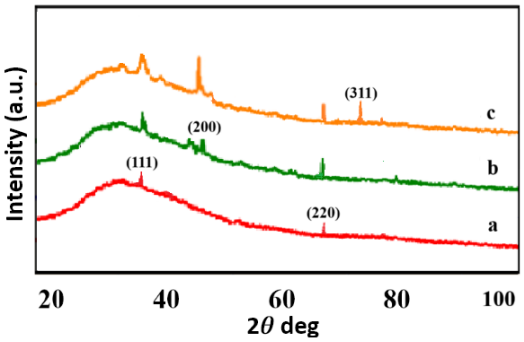

Fig. 2. X-ray diffraction (XRD) patterns of the top (A) and bottom (B) surfaces for (a) AgNH, (b) 0.33 mmol/g AgNH-PVS, and (c) 0.63 mmol/g AgNH-PVS samples.

Overall, the development of the Ag_2S phase is predominantly confined to the surface regions of the nanocomposite, where the diffusion of H_2S is more effective. The formation of this phase is accompanied by noticeable structural transformations, which are indicative of phase transitions occurring as a result of the chemical interaction between silver ions and hydrogen sulfide. These observations provide valuable insight into the diffusion behavior and surface reactivity of silver-containing polymer nanocomposites under gaseous sulfur environments.

Figure 3 presents the optical absorption spectra of sulfided AgNPs-PVA nanocomposites. The experimental results depicted in the optical spectra clearly demonstrate that upon exposure to H_2S gas, the surface plasmon resonance (SPR) of silver nanoparticles (AgNPs) is significantly attenuated. This attenuation is primarily attributed to the chemical interaction between H_2S gas and the surface of Ag NPs, leading to the formation of the Ag_2S phase. Such a transformation alters the surface structure of the Ag nanoparticles, consequently diminishing their plasmonic properties and reducing the collective oscillation frequency of conduction electrons. It is important to note, however, that not all nanoparticles embedded within the nanocomposite react uniformly with H_2S gas. One of the main reasons for this inhomogeneous reaction is that only one side of the nanocomposite is directly exposed to H_2S. As a result, only the silver nanoparticles located on the bottom surface undergo significant sulfuration, while the others largely retain their original optical characteristics. This partial sulfuration explains why the plasmon resonance

peaks do not vanish completely but instead show a reduction in overall absorption intensity. Moreover, the surface activity of the nanoparticles and the diffusion properties of the surrounding medium also play crucial roles in determining the reaction kinetics. These optical properties are tunable, as the Ag_2S layers formed at the bottom of the Ag nanocomposite possess a higher refractive index (1.9–2.5) and a higher relative dielectric constant ($\varepsilon_r \approx 6$) compared to pure Ag [9]. It is well-established that the localized surface plasmon resonance (LSPR) of silver nanoparticles is highly sensitive to changes in the surrounding dielectric environment. The formation of Ag_2S layers on the surface of Ag nanoparticles modifies this dielectric environment, thereby enabling dynamic tuning of the plasmonic response [10].

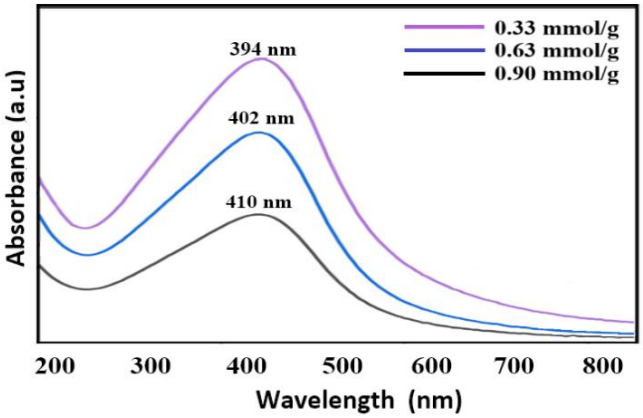

Fig. 3. Absorption spectrum of sulfided AgNPs-PVA nanocomposites at concentrations of 0.33 mmol/g, 0.63 mmol/g, and 0.90 mmol/g.

As previously noted, exposure to H_2S gas induces significant alterations in the optical properties of the samples, most notably observed as a redshift in the plasmon resonance peaks. This shift in plasmon resonance frequency is strongly correlated with the concentration of free electrons and can be interpreted within the framework of the Drude model, which accurately describes the behavior of free electron systems [11]. The observed redshift corresponds to an increase in the resonance wavelength and, consequently, a decrease in the plasmon resonance frequency. This phenomenon is attributed to a reduction in the free electron concentration, which is likely caused by chemical modifications occurring under the influence of H_2S gas. The relationship between the change in plasmon resonance frequency and the concentration of free electrons is quantitatively described by Equation (1).

$$\omega = \sqrt{ne^2/\varepsilon_0 m^*} \quad (1)$$

According to equation (1), the plasmon resonance frequency ω_p is determined by the concentration of free electrons n, the elementary charge (e), the vacuum permittivity ε_o, and the effective mass of the electrons m^*. In the nanocomposite under study, the Ag nanoparticles embedded within the matrix undergo a surface reaction with H_2S gas, leading to the formation of a semiconducting Ag_2S phase on their surface. Since Ag_2S is a semiconductor, it possesses a significantly lower free electron concentration compared to metallic Ag nanoparticles. As a result, the formation of Ag_2S leads to a reduction in the overall free electron density in the system, causing a redshift in the localized surface plasmon resonance (LSPR) towards longer wavelengths. Furthermore, the Ag_2S layer formed at the semiconductor-metal interface acts as a screening medium for the incident electromagnetic waves, thereby attenuating the interaction between the external field and the free electrons of the metallic Ag core. This screening effect decreases the electron density available for plasmonic excitation, resulting in a notable reduction in both the intensity and spectral position of the LSPR peak. These findings illustrate a progressive isolation of the Ag nanoparticles, which weakens their collective interaction with the incident electromagnetic radiation. This transformation significantly affects the electrical and optical properties of the Ag nanostructures. The observed decrease in carrier tunneling across the system can be attributed to the increasing thickness and semiconducting nature of the Ag_2S layer, which serves as a barrier to charge transport. The calculated concentrations of sulfide-modified AgNPs–PVA nanocomposites at different H_2S exposures are summarized in Table 1, providing quantitative insight into the extent of this chemical transformation and its impact on the plasmonic behavior.

Table 1. LSPR Peak, Carrier Concentration, and Band Gap of AgNPs–PVA

Sample	Plasmon Resonance Peak (nm)	Free Electron Concentration (cm^{-3})	Band Gap Energy (eV)
AgNPs-PVA (0.33 mmol/g)	394	$7{,}19\times10^{24}$ cm^{-3}	2,3
AgNPs-PVA (0.63 mmol/g)	402	$6{,}91\times10^{24}$ cm^{-3}	2,11
AgNPs-PVA (0.90 mmol/g)	410	$6{,}64\times10^{24}$ cm^{-3}	2,03

There is a significant difference in the arrangement of energy levels between bulk materials and nanomaterials. Nanomaterials exhibit a larger band gap and consist of more discrete energy levels. This observed distinction can be attributed to various quantum confinement effects present in nanoparticles, which typically measure only a few nanometers in size—equivalent to several atomic layers. Generally, the optical band gap energy in metals is determined by plotting $(\alpha(h\nu))^{1}/^{m}$ versus photon energy (hν), where α(ν) represents the absorption coefficient, and

m indicates the type of electronic transition. The value of m can vary: 1/2 corresponds to allowed direct transitions, 2 to allowed indirect transitions, 3/2 to forbidden direct transitions, and 3 to forbidden indirect transitions.

As shown in Figure 4, the band gap values for AgNPs-PVA nanocomposites vary with silver nanoparticle concentration: 2.3 eV at 0.33 mmol/g, 2.11 eV at 0.63 mmol/g, and 2.03 eV at 0.90 mmol/g. Upon exposure to H_2S gas, silver nanoparticles undergo a sulfidation reaction, forming Ag_2S on their surface. The kinetics of this reaction are primarily governed by the surface area of the nanoparticles and the diffusion rate of H_2S. Smaller particles, having a larger specific surface area, facilitate a faster reaction rate. However, as the Ag_2S layer thickens, it imposes a diffusion barrier, gradually slowing down the reaction. At higher silver concentrations,

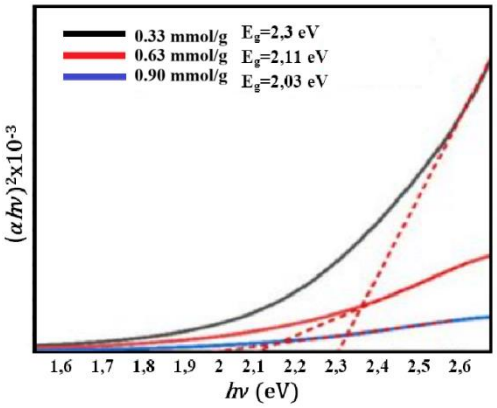

Fig. 4. Band gap energies of the sulfided nanocomposites at concentrations of 0.33 mmol/g, 0.63 mmol/g, and 0.90 mmol/g.

the sulfidation proceeds more rapidly, leading to increased formation of Ag_2S. Consequently, the thickness of the Ag_2S layer increases with the mass concentration of AgNPs. At a concentration of 0.33 mmol/g, only a limited amount of Ag_2S forms on the surface of the silver nanoparticles, resulting in a relatively wider band gap of 2.3 eV. In contrast, at 0.63 mmol/g and 0.90 mmol/g, more substantial Ag_2S formation occurs, narrowing the band gap to 2.11 eV and 2.03 eV, respectively. The formation of Ag_2S is associated with a decrease in the band gap of the Ag nanoparticles due to the different electronic structure of Ag_2S compared to pure silver. As the number of Ag_2S ions increases, the quantum size effects of silver diminish, leading to a further reduction in the band gap. According to the literature, the band gap of Ag_2S nanocrystals typically falls within the range of 0.9–1.1 eV [12]. Therefore, spectral analysis confirms that sulfur incorporation induces modifications in the band structure of Ag–Ag_2S core–shell heterostructures. This can be attributed to the efficient transfer of photoexcited electrons from the conduction band of Ag_2S

to that of metallic Ag at the Ag–Ag_2S interface. The formation of Ag–Ag_2S heterojunctions alters the band alignment at the interface, promotes charge separation, and suppresses charge carrier recombination. The band gap values for the sulfided samples were determined using the Tauc method.

$$(\alpha h\nu)^2 = A\big(h\nu - E_g\big). \quad (2)$$

The photon energy, denoted as $h\nu$, is a constant dependent on the structure and type of the sample. E_g represents the band gap, and n is a factor that varies depending on the type of transition: for a direct allowed transition, n=2, while for an indirect allowed transition,

α is the absorption coefficient, which is derived from the Beer-Lambert law. Additionally, the increase in the Ag_2S content within the forbidden band significantly reduces with respect to the interaction between Ag_2S nanoparticles and polymer chains. This interaction leads to a decrease in the Fermi level [13]. The reduction in the Fermi level, in turn, affects the energy gap. Another contributing factor is the increased degree of disorder in the crystal lattice, which causes an expansion of energy bands in localized electron states [14].

4. Conclusion

In this study, silver nanoparticles (AgNPs) were successfully synthesized via a chemical reduction method and subsequently incorporated into polyvinyl alcohol (PVA) to fabricate AgNPs/PVA nanocomposites with varying molar concentrations of silver nanoparticles: 0.33 mmol/g, 0.63 mmol/g, and 0.90 mmol/g. The prepared nanocomposites were exposed to H_2S gas unidirectionally, after which both surfaces of the composite were systematically analyzed. Structural analyses revealed that the AgNPs on the exposed surface underwent sulfidation, resulting in the formation of Ag_2S. Concurrently, chain scission in the polymer matrix was observed, leading to a decrease in the degree of crystallinity. Importantly, the extent of these structural changes was found to be dependent on the concentration of AgNPs within the nanocomposites. Higher concentrations facilitated greater interactions between Ag^+ ions and H_2S gas, promoting more extensive formation of Ag_2S. X-ray diffraction (XRD) analysis corroborated these findings, exhibiting characteristic diffraction peaks corresponding to AgNPs/PVA nanocomposites, with increased peak intensity on the surface exposed to H_2S gas. Additionally, UV-Vis spectroscopy demonstrated a reduction in the intensity of the localized surface plasmon resonance (LSPR) peaks along with a red shift, attributed to the diminished free electron density as AgNPs transformed into Ag_2S. Additionally, the observed reduction in the optical band gap (Eg) to as low as 2.03 eV is attributed to the formation of Ag_2S nanocrystals within the nanocomposite. Collectively, these results confirm that the

proposed approach enables the successful fabrication of asymmetric nanostructured composites. The observed dependence on nanoparticle concentration provides valuable insights for tuning structural and optical properties in response to gaseous stimuli, suggesting promising potential for future applications in sensing and responsive material systems.

References

[1] Su, Shei Sia, and Isaac Chang. "Review of production routes of nanomaterials." Commercialization of nanotechnologies–a case study approach (**2018**): 15-29.

[2] M. Zannotti, V. Vicomandi, A. Rossi et al., "Tuning of hydrogen peroxide etching during the synthesis of silver nanoparticles. An application of triangular nanoplates as plasmon sensors for Hg^{2+} in aqueous solution," *Journal of Molecular Liquids*, vol. 309, article 113238, **2020**.

[3] Abdulkadir, B. A., Dennis, J. O., Abd Shukur, M. F. B., Nasef, M. M. E., & Usman, F. (**2021**). Study on dielectric properties of gel polymer electrolyte based on PVA-K_2CO_3 composites. International Journal of Electrochemical Science, 16(1), 150296.

[4] Abdallah O.M., EL-Baghdady K.Z., Khalil M.M., El Borhamy M.I., Meligi G.A. Antibacterial, antibiofilm and cytotoxic activities of biogenic polyvinyl alcohol-silver and chitosan-silver nanocomposites. *J. Polym. Res.* **2020**;27:1–9.

[5] Boyetey, M. J. B., Torgbo, S., & Sukyai, P. (**2023**). Bio-scaffold for bone tissue engineering with focus on bacterial cellulose, biological materials for hydroxyapatite synthesis and growth factors. *European Polymer Journal*, *194*, 112168.

[6] Pattnaik, C., Mishra, R., Sahu, A. K., Sahoo, L. N., Sahoo, N. K., Tripathy, S. K., & Sahoo, S. (**2023**). Green synthesis of glucose-capped stable silver nanoparticles: a cost-effective sensor for the selective detection of Hg 2+ ions in aqueous solutions. *Sensors & Diagnostics*, *2*(3), 647-656.

[7] Lu, J., Liu, D., & Dai, J. (**2019**). Preparation of highly conductive silver nanowires for electrically conductive adhesives. Journal of Materials Science: Materials in Electronics, 30(16), 15786-15794.

[8] Sahraoui, K., Benramdane, N., Khadraoui, M., Miloua, R., & Mathieu, C. (**2014**). Characterization of silver sulphide thin films prepared by spray pyrolysis using a new precursor silver chloride. Sensor s & Transducers, 27, 319-325

[9] Jiang, Qian, Wenxia Zeng, Canying Zhang, Zhaoguo Meng, Jiawei Wu, Qunzhi Zhu, Daxiong Wu, and Haitao Zhu. "Broadband absorption and enhanced photothermal conversion property of octopod-like Ag@ Ag2S core@ shell structures with gradually varying shell thickness." Scientific Reports 7, no. 1 (**2017**): 17782.

[10] Rycenga, Matthew, Claire M. Cobley, Jie Zeng, Weiyang Li, Christine H. Moran, Qiang Zhang, Dong Qin, and Younan Xia. "Controlling the synthesis and assembly of silver

nanostructures for plasmonic applications." Chemical reviews 111, no. 6 (**2011**): 3669-3712.

[11] M. B. Gebeyehu, T. F. Chala, S. Y. Chang, C. M. Wu and J. Y. Lee, *RSC Adv.*, **2017**, 7(26), 16139–16148

[12] R. Zamiri, H. Abbastabar Ahangar, A. Zakaria, G. Zamiri, M. Shabani, B. Singh and JMF Ferreira, *Chem. sent. J.* , **2015**, 9 (1), 1–6

[13] Rozra, Jyoti, Isha Saini, Annu Sharma, Navneet Chandak, Sanjeev Aggarwal, Rajnish Dhiman, and Pawan K. Sharma. "Cu nanoparticles induced structural, optical and electrical modification in PVA." Materials Chemistry and Physics 134, no. 2-3 (**2012**): 1121-1126.

[14] El-Mansy, M. K., E. M. Sheha, K. R. Patel, and G. D. Sharma. "Characterization of PVA/CuI polymer composites as electron donor for photovoltaic application." Optik 124, no. 13 (**2013**): 1624-1631.